ARTICLE IN PRESS

Applied Mathematical Modelling xxx (2013) xxx–xxx

Contents lists available at SciVerse ScienceDirect

Applied Mathematical Modelling

journal homepage: www.elsevier.com/locate/apm

Modeling the asymmetry in traffic flow (a): Microscopic approach

Hao Xu [1], Hongchao Liu *, Huaxin Gong [2]

Department of Civil & Environmental Engineering, Texas Tech University, Lubbock, TX 79409-1023, United States

ARTICLE INFO

Article history:
Available online xxxx

Keywords:
Asymmetric car-following
Microscopic model
Anisotropic

ABSTRACT

The asymmetric characteristic of a vehicle's ability in deceleration and acceleration, as well as its impact to micro- and macroscopic traffic flow has caused increased attention from both theoretical and practical sides. However, how to realistically model this property remains a challenge to researchers. This paper is one of the two studies on this topic, which is focused on the modeling at the microscopic level from the investigation of car-following behavior. The second part of the study [H. Liu, H. Xu, H. Gong, Modeling the asymmetry in traffic flow (b): macroscopic approach, Appl. Math. Model. (submitted for publication)] is focused on the modeling of this asymmetric property from the macroscopic scale. In this paper, we first present an asymmetric full velocity difference car-following approach, in which a higher order differential equation is developed to take into account the effect of asymmetric acceleration and deceleration in car-following. Then, efforts are dedicated to calibrate the sensitivity coefficients from field data to complete the theoretical approach. Using the data recorded from the main lane traffic and ramp traffic of a segment of the US101 freeway, the two sensitivity coefficients have been successfully calibrated from both congested and light traffic environments. The experimental study reveals that in the studied traffic flow, the intensity of positive velocity difference term is significantly higher than the negative velocity difference term, which agrees well with the results from studies on vehicle mechanics.

1. Introduction

Research on the car-following behavior attempts to reveal, at the microscopic scale, the interactions between vehicle pairs in a traffic stream without making lane changes. The performance of car-following models relies greatly on realistically modeling the interaction terms between individual vehicles under varying traffic circumstances. As car-following is a fundamental driving behavior which has significant impact on both highway mobility and traffic safety, it has been studied extensively from both theoretical and data-driven approaches [2].

Mathematical modeling has been widely applied in transportation to depict the characteristics of traffic movement for best control and operation of highway facilities, such as the recent work of Wang et al. [3] in which a discrete Markov chain process was used to calculate the probability of traffic breakdowns, and Gu et al. [4] who models the capacity of highway checkpoints with unconventional configurations. Pioneering studies in car-following theories include, but are not limited to, the works of Herman et al. [5] and Newell [6] who tackled the problem from vehicle dynamics, and Tian et al., who investigated the driver's critical gap [7]. Recent improvements include the work of Bando et al. [8], in which an optimal

* Corresponding author. Tel.: +1 (806) 742 2801.
E-mail addresses: hao.xu@ttu.edu (H. Xu), hongchao.Liu@ttu.edu (H. Liu), flowdynamic@gmail.com (H. Gong).
[1] Tel.: +1 (806) 742 3523.
[2] Tel.: +1 (806) 786 0934.

0307-904X/$ - see front matter © 2013 Elsevier Inc. All rights reserved.
http://dx.doi.org/10.1016/j.apm.2013.04.037

velocity (OV) approach was proposed to take into account a driver's intention to maintain its optimal velocity in the traffic stream; the general force (GF) model by Helbing and Tilch [9], which addresses the issue of unrealistically high acceleration and deceleration found in the OV approach; and the work by Jiang et al. [10], which extended the GF approach to the full velocity difference (FVD) model that took the full velocity difference into account.

However, the existing car-following models have not sufficiently taken the asymmetry of acceleration and deceleration behaviors into consideration. In reality, a vehicle's ability in deceleration is higher than acceleration, as demonstrated in [6,7]. This asymmetric characteristic and its impacts on traffic flow have been investigated by researchers, for instance, in [11,12] traffic flow was presented differently in state of acceleration, deceleration and equilibrium to demonstrate the difference. Kim and Zhang further proposed a new stochastic wave propagation model that can distinguish the acceleration wave with a smaller speed, the acceleration wave with a larger speed, and the deceleration wave with both smaller and larger speed [13,14]. In this regard, further investigation of car-following behavior could also help to improve the quality of continuum models.

Owing to its inherent nature of microscopic scale study of individual vehicles, very few of the recent car-following mathematical models have been validated against field data. Special experimental studies were designed by a handful of researchers. For instance, Ranjitkar et al. [15] recorded vehicle trajectory data from ten passenger cars equipped with Global Positioning System (GPS) receivers; Brockfeld et al. [16] and Punzo and Simonelli [17] used differential GPS (DGPS) to extract vehicle trajectories; Ossen and Hoogendoorn [18] used high-resolution digital images from a helicopter; and Fouladvand and Darooneh [19] analyzed the time series of velocity, velocity difference, spatial gap and the acceleration using the field data. Unfortunately, these studies were conducted on a project basis and the data were discarded upon completion of a specific study, instead of making it publicly available.

Besides the mathematical modeling, another challenging problem faced in this research is to use real-world data that is publicly available to capture the asymmetric characteristics of individual vehicles in the traffic stream and use the data to validate the mathematic model. The dataset used in the experimental test is from the Next Generation SIMulation (NGSIM) project, which was funded by the Federal Highway Administration for the purpose of validating and calibration of microscopic simulation models.

In this paper, the authors first depict the fundamental relationship among the classical and two state-of-the-art car-following models, namely, the OV and the GF model. The purpose of the in-depth analysis of these models is to lay a logical ground for the discussion of the asymmetric full velocity difference (AFVD) model and the calibration process. With the mathematical modeling approach described, attentions are then directed to the experimental study, in which the authors demonstrate the mechanism and process to extract the asymmetric sensitivity coefficients from the vehicle trajectories in the NGSIM dataset. In the end, the sensitivity coefficients derived from the field data are introduced into simulation experiments to demonstrate the enhanced realism of the asymmetric AFVD model through a comparison with the symmetric FVD model.

2. The optimal velocity theory and its recent improvements

Car-following models are designed to describe the behavior of individual drivers in a stream of interacting vehicles without making lane changes. Classic models describe the movement of the nth vehicle following a leading $(n-1)$th vehicle as follows

$$\frac{dv_n}{dt}(t+\Delta t) = \lambda \Delta v \tag{1}$$

where $\Delta v = v_{n-1}(t) - v_n(t)$ and Δt is the time lag of response, λ is the sensitivity. Applying the classic model, one can describe a vehicle's movement as a function of the leading vehicle's trajectory. In addition, it allows us to establish a bridge between microscopic car-following studies and macroscopic continuum models. In 1995, an optimal velocity (OV) theory was proposed by a group of Japanese researchers, which models car-following differently. The OV model is based on the idea that vehicles adapt to a distance-dependent optimal velocity in car-following. It accounts for the effect of time lag through the second order differential equations based on the equation of motion in physics. Therefore, the time lag in the OV model is not the delay from driver's response, but the delay of car motion which has its root in the dynamic equation itself. Their model reads

$$\frac{dv_n(t)}{dt} = \kappa[V(\Delta X_n(t)) - v_n(t)] \tag{2}$$

where n is the following vehicle, V is the optimal velocity function and κ is the sensitivity coefficient. Despite its simplicity, the OV model overcomes the problems found in classic models and realistically describes several critical properties of traffic flows such as stop-and-go waves and the evolution of traffic congestion.

Helbing and Tilch [9] found the OV model might result in questionable high acceleration and unrealistic deceleration under certain circumstances and modified it into a general force (GF) model, which is expressed by

$$\frac{dv_n}{dt} = \frac{v_n^0 - v_n}{\tau_n} + f_{n,n-1}(x_n,\ v_n;\ x_{n-1},\ v_{n-1}) \tag{3}$$

where $f_{n,n-1}$ is the "force" and expressed by

$$f_{n,n-1} = \frac{V(s_n) - v_n^0}{\tau_n} - \frac{\Delta v_n \Theta(\Delta v_n)}{\tau_n'} e^{-[s_n - s(v_n)]/R_n'} \tag{4}$$

in which, v_n^0 is the desired optimal velocity; Θ is the Heaviside function and $\tau_n = 1/\kappa$ is the acceleration time. τ'_n is the braking time, which should be smaller than τ_n. s_n is the distance between two vehicles. R'_n can be interpreted as the range of the braking interaction. $s(v_n)$ denotes the velocity-dependent safe distance.

As the GF model only investigated the case where the velocity of the following vehicle is larger than that of the leading vehicle, Jiang et al. [10] pointed out that when the leading vehicle is much faster, the following vehicle may not brake even though the spacing is smaller than the safe distance. Considering both positive and negative velocity differences, they proposed a full velocity difference (FVD) approach as follows:

$$\frac{dv_n(t)}{dt} = \kappa[V(s) - v_n(t)] + \lambda\Delta v \tag{5}$$

Because the GF model does not consider the contribution of the positive Δv to the vehicle interaction, the FVD made a slight modification on the interaction term to address this issue.

3. The asymmetric full velocity difference (AFVD) approach

The optimal velocity approach and the aforementioned improvements are remarkable achievements in recent car-following studies, however, they are not without drawbacks. First, the asymmetric characteristic in acceleration and deceleration was not sufficiently considered. The idea of adding a higher order term to the OV model to precisely address vehicular interactions provides a great opportunity to model the asymmetric property in car-following, unfortunately, this has not been adequately addressed in the GF model. If one simplifies Eqs. (3) and (4), the GF model can be expressed by

$$\frac{dv_n}{dt}(t) = \kappa[V(s) - v_n(t)] + \lambda\Theta(-\Delta v)\Delta v \tag{6}$$

where Θ is the Heaviside function and $V(s)$ is the optimal velocity and s is the spacing. The GF model adopted the fundamental form of the OV model but added a term on the right hand side of Eq. (2) to precisely model vehicular interactions. Eq. (6) could be easily extended to an asymmetric full velocity difference (AFVD) approach in which we can define two sensitivity coefficients to separately model the positive and negative velocity [11]. Such a model can be expressed by

$$\frac{dv_n}{dt}(t) = \kappa[V(\Delta x_n(t)) - v_n(t)] + \lambda_1 H(-\Delta v_n(t))\Delta v_n(t) + \lambda_2 H(\Delta v_n(t))\Delta v_n(t) \tag{7}$$

where H is the Heaviside function.

Next, we are interested in getting the mathematical presentation of λ_1 and λ_2 from the presentation of λ in the GF model. Let's rewrite the GF model in a different form

$$\frac{dv_n}{dt} = \frac{V_n^*(s_n, v_n, \Delta v_n) - v_n(t)}{\tau_n^*} \tag{8}$$

where s_n, v_n and Δv_n are spacing, velocity, and velocity difference, respectively. τ_n^* is the optimal τ_n given by

$$\frac{1}{\tau_n^*} = \frac{1}{\tau_n} + \frac{\Theta(\Delta v_n)}{\tau''_n} \tag{9}$$

where

$$\tau''_n = \tau''_n \exp\{[s_n - s(v_n)]/R'_n\} \tag{10}$$

The optimal velocity, V_n^*, can be represented by

$$V_n^* = \frac{\tau''_n V_n + \tau_n\Theta(\Delta v_n)v_{n-1}}{\tau''_n + \tau_n\Theta(\Delta v_{n)}} \tag{11}$$

if one substitutes Eq. (11) into Eq. (8), we can get

$$\begin{aligned}
\frac{dv_n(t)}{dt} &= \frac{V_n^*(s_n, v_n, \Delta v_n) - v_n(t)}{\tau_n^*} = \frac{\frac{\tau''_n V_n(s_n, v_n) + \tau_n\Theta(\Delta v_n)v_{n-1}(t)}{\tau''_n + \tau_n\Theta(\Delta v_n)} - v_n(t)}{\tau_n^*} \\
&= \left[\frac{\tau''_n V_n(s_n, v_n) + \tau_n\Theta(\Delta v_n)v_{n-1}(t)}{\tau''_n + \tau_n\Theta(\Delta v_n)} - v_n(t)\right]\left(\frac{1}{\tau_n} + \frac{\Theta(\Delta v_n)}{\tau''_n}\right) \\
&= \frac{\tau''_n V_n(s_n, v_n) + \tau_n\Theta(\Delta v_n)v_{n-1}(t)}{\tau''_n + \tau_n\Theta(\Delta v_n)} \cdot \frac{\tau''_n + \tau_n\Theta(\Delta v_n)}{\tau_n\tau''_n} - v_n(t)\left(\frac{1}{\tau_n} + \frac{\Theta(\Delta v_n)}{\tau''_n}\right) \\
&= \frac{V_n(s_n, v_n)}{\tau_n} + \frac{v_{n-1}(t)\Theta(\Delta v_n)}{\tau''_n} - \frac{v_n(t)}{\tau_n\Theta} - \frac{v_n(t)\Theta(\Delta v_n)}{\tau''_n} = \frac{V_n(s_n, v_n) - v_n(t)}{\tau_n} - \frac{v_n(t) - v_{n-1}(t)}{\tau''_n}\Theta(\Delta v_n) \\
&= \frac{V_n(s_n, v_n) - v_n(t)}{\tau_n} - \frac{\Delta v_n}{\tau''_n}\Theta(\Delta v_n)
\end{aligned} \tag{12}$$

which gives

$$\lambda = \frac{1}{\tau''_n} = \frac{1}{\tau'_n \exp\{[s_n - s(v_n)]/R'_n\}} \tag{13}$$

Therefore, in the asymmetric full velocity difference model, λ takes the following forms

$$\lambda_1 = \frac{1}{\tau'_n} e^{-[s_n - s(v_n)]/R'_n} \tag{14}$$

$$\lambda_2 = \frac{1}{\tau'''_n} e^{-|s_n - s(v_n)|/R''_n} \tag{15}$$

in which, τ'''_n and R'_n are two new parameters obtained during the mathematical derivation which need to be determined by field data.

Fig. 1 explains the significance of representing acceleration and deceleration by two sensitivity coefficients. The curve on the top represents the relationship between the space-headway and the intensity of acceleration, with the point S being the minimum comfortable safe distance for the following vehicle. The curve on the bottom demonstrates a similar relationship between the intensity of deceleration and the space-headway. From the figure, one can find that the intensity of acceleration and deceleration both decreases as the headway increases when headway is larger than the minimum comfortable following distance, which implies that the interaction intensity will become zero while the space headway reaches infinity. However, when the space-headway is smaller than the safe distance, the intensity of deceleration increases sharply as the space headway decreases, which is depicted by the deceleration curve.

The stability condition for the AFVD model could be defined as in [19], which is:

$$f = V'(b) \begin{cases} < \frac{\kappa}{2} + \lambda_1 & \textit{when } \Delta v_n < 0 \\ < \frac{\kappa}{2} + \lambda_2 & \textit{when } \Delta v_n > 0 \end{cases} \tag{16}$$

Note that in the FVD model, the stability condition is

$$f = V'(b) < \frac{\kappa}{2} + \lambda \tag{17}$$

in the OV model, it is

$$f = V'(b) < \frac{\kappa}{2} \tag{18}$$

Therefore, the OV model, the GF model and the FVD model can all be presented by the AFVD model as its special cases. If one defines $\lambda_1 = \lambda_2 = \lambda$, the AFVD model represents the FVD model, while when $\lambda_1 = \lambda_2 = \lambda = 0$, both the AFVD model and the FVD model becomes the OV model.

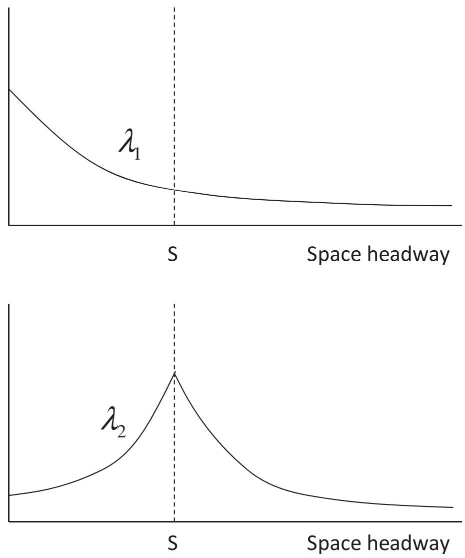

Fig. 1. Relationship between the two sensitivity coefficients and the space headway.

4. Calibration of the sensitivity coefficients using the NGSIM dataset

Adding a higher order term and additional sensitivity coefficients to precisely model the vehicular interaction is a fundamental improvement to the optimal velocity theory. These modifications, though simple, have greatly improved the model's performance. The calibration in Helbing and Tilch [9] shows that in the general force model $\kappa = 0.41/\mathrm{s}$, which is much smaller than that in OV, which is 0.85/s, and thus overcome the over acceleration problem. The new sensitivity coefficient λ, however, has not been calibrated against field data. For instance, in Jiang et al. [8], it was found that the value of λ has a significant impact to the size of the hysteresis loop and the status of stability. Not knowing the practical values of λ, the authors used a set of hypothetical λ values to show this impact, which resulted in an unrealistic phenomenon in which a λ value of 0.4 corresponds to a negative speed. Is $\lambda = 0.4$ a realistic value? How to calibrate λ values from a traffic stream other than from a few vehicles with specific devices?

In this section, the authors use real vehicle trajectory data from massive traffic flows to calibrate the two sensitive coefficients in AFVD in both congested and light traffic conditions. The authors first took Helbing and Tilch's calibration process and applied a standard nonlinear regression approach to calibrate κ in the GF model to examine the quality of the screened data and the effectiveness of the calibration method. Then, same process was used to calibrate λ_1 and λ_2 of the AFVD model using both main lane and ramp data.

4.1. The next generation simulation (NGSIM) vehicle trajectory dataset

The NGSIM project was funded by the Federal Highway Administration (FHWA) for the development and validation of microscopic traffic simulation models. Video data at an interval of 0.1 s have been collected from various sites in the United States. In this study, the data from a 2100 feet 5-lane segment of the U.S. 101 Freeway (see Fig. 2) was used. The processed data has each single vehicle's identification number, time frame number, relative spatial coordinates, vehicle properties (length, width, class, velocity, acceleration), lane identification, preceding and following vehicle numbers, and both space and time headways.

4.2. Calibration using main lane traffic

The traffic data of the innermost lane (lane 1, the farthest lane from on and off ramps) was utilized to minimize the impacts caused by lane changing. A time-space diagram was first developed to examine the quality of

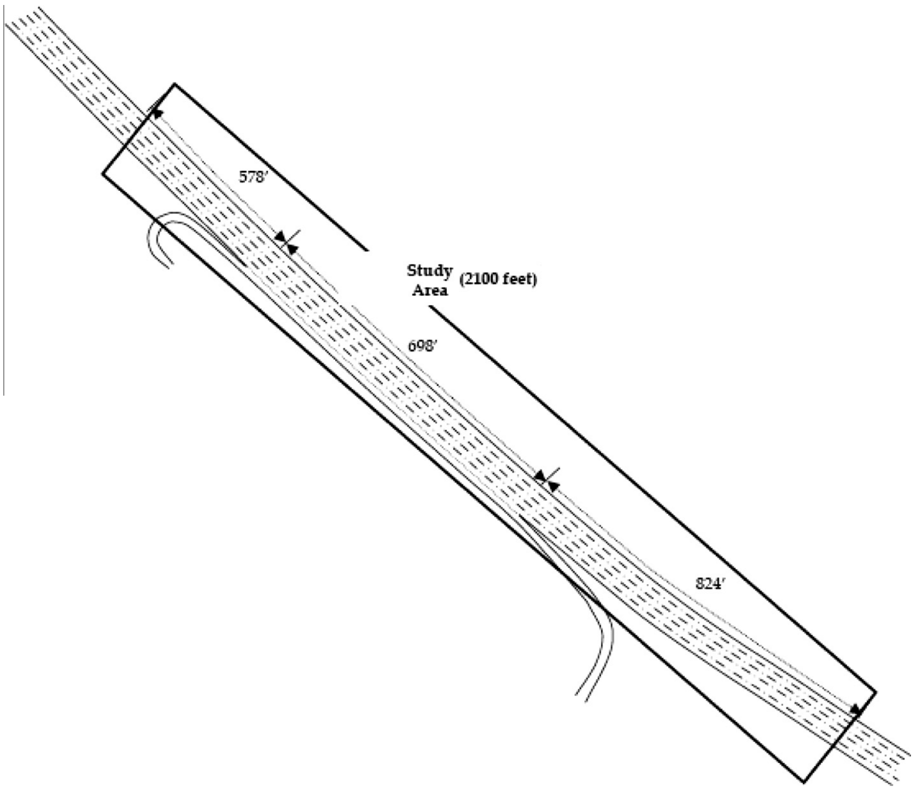

Fig. 2. The schematic of the study site – a segment of U.S. 101.

Please cite this article in press as: H. Xu et al., Modeling the asymmetry in traffic flow (a): Microscopic approach, Appl. Math. Modell. (2013), http://dx.doi.org/10.1016/j.apm.2013.04.037

the data. As shown in Fig. 3, the sample data reflects apparent dynamics and clear shock wave propagation activity.

The data are further screened according to the criteria set in Table 1 for car-following analysis. The filtered data is then used in a nonlinear regression approach to first calibrate κ in the GF model. We have demonstrated in previous sections that both FVD and AFVD models have their roots in the general force approach but use different higher order terms to more precisely model the vehicular interaction. If the data screening and calibration process is correct, the κ value in FVD and AFVD should be very close to that in the GF model.

The nonlinear regression method used in this study is a special form of the least squares analysis, which is often used to fit a set of m observations with a model that is non-linear with n unknown parameters ($m > n$). The basis of the method is to approximate the model by a linear process and to refine the parameters by successive iterations. A primary assumption underlying this procedure is that the model can be approximated by a linear function.

$$f(x_i, \beta) \approx f^0 + \sum_j J_{ij}\beta_j \tag{19}$$

where $J_{ij} = \frac{\partial f(x_i,\beta)}{\partial \beta_j}$ and the least squares estimators are therefore given by $\hat{\beta} \approx (J^T J)^{-1} J^T y$. As it is a standard regression process, detailed description is not provided in the manuscript, interested readers are encouraged to refer to Mathematica.

In the following we first examine the method by applying it to the GF model to calibrate κ and other constants, which yields,

$$\frac{dv_n(t)}{dt} = \kappa[Tanh(b\Delta x_n(t) - c) - v_n(t)] \tag{20}$$

The regression result from the screened data of the lane 1 traffic in 7:50–8:05 AM gives

$$\frac{dv_n(t)}{dt} = 0.415873[Tanh(1.80049\Delta x_n(t) - 10.4075) - v_n(t)] \tag{21}$$

in which $\kappa = 0.415873\ s^{-1}$ agrees well with the result in Helbing and Tilch (1998). The result thus proved the validity of the calibration method and examined the quality of the filtered data.

Next, we further run the same nonlinear regression by separately using the positive velocity difference data and the negative velocity difference data, which is the case in the full velocity difference approach. The result is shown in Table 2 along with the result from the general calibration process described in Section 4.1.

Similarly, the quantitative values as well as the relative relation between the accelerating and decelerating sensitivity coefficients in the asymmetric AFVD model could be obtained using the same method, which gives

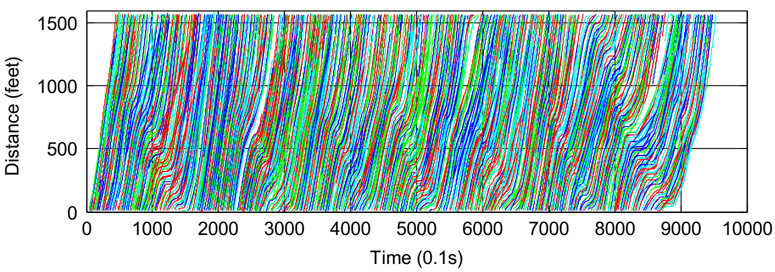

Fig. 3. The time space diagram for lane 1 of U.S. 101 (7:50–8:05 AM).

Table 1
Data screening criteria for car-following analysis of the lane 1 traffic.

Velocity	>=	5 ft/s
Spacing	<=	120 ft
Headway	<=	20 s
Velocity difference	>=	1 ft/s
Vehicle class		Auto

Table 2
Calibration of the full velocity difference model (FVD) using the lane 1 traffic data.

General	$\frac{dv_n(t)}{dt} = 0.415873[Tanh(1.80049\Delta x_n(t) - 10.1075) - v_n(t)]$
$\Delta v_n(t) > 0$	$\frac{dv_n(t)}{dt} = 0.450816[Tanh(0.000663492\Delta x_n(t) - 16.5936) - v_n(t)]$
$\Delta v_n(t) < 0$	$\frac{dv_n(t)}{dt} = 0.384879[Tanh(1.84944\Delta x_n(t) - 10.5018) - v_n(t)]$

Please cite this article in press as: H. Xu et al., Modeling the asymmetry in traffic flow (a): Microscopic approach, Appl. Math. Modell. (2013), http://dx.doi.org/10.1016/j.apm.2013.04.037

$$\frac{dv_n(t)}{dt} = 0.415873 \quad [Tanh(1.80049\Delta x_n(t) - 10.4075) - v_n(t)] + 1.0824H(-\Delta v_n(t))\Delta v_n(t) + 0.69271H(-\Delta v_n(t))\Delta v_n(t) \tag{22}$$

This reveals that under the given traffic condition, the decelerating and accelerating sensitivity coefficients are 1.0824 and 0.69271, respectively, which indicates a relative relation of 1.56 between the intensity of deceleration and acceleration.

4.3. On-ramp and off-ramp traffic

Experimental analysis thus far has successfully calibrated the accelerating and decelerating sensitivity coefficients in AFVD using the main lane data which represents the case of dense traffic condition. We are also interested in identifying the upper boundary of the difference of λ_1 and λ_2, i.e., $|\lambda_1/\lambda_2|$ and their values in light traffic. Vehicles at on and off ramps of the study site provides an ideal circumstance for this purpose due to the skewed distribution of acceleration and deceleration at on and off ramps.

The length of the on-ramp and off-ramp is 193 ft and 143 ft, respectively. Table 3 shows the screening criteria to ensure the selected data are in car-following mode. The criteria are the same as in the main lane analysis except the spacing is less than 60 ft considering the length of the ramps. Figs. 4 and 5 are the time-space diagrams from the screened data (in 0.1 s time frame), which show light traffic conditions on both on- and off-ramps.

The analysis of the ramp data is focused on calibrating the values of λ_1 and λ_2 in the AFVD model. Using the same non-linear regression process, the sensitivity coefficients of on- and off-ramp traffic are obtained. Table 4 shows the results of the calibration along with that from the main lane data.

From the off-ramp traffic, which features collective decelerating behavior, the values of the sensitivity coefficients for deceleration and acceleration are 0.997205 and 0.361254, respectively. While from the on-ramp segment that features weighted acceleration, the sensitivity coefficients are found to be 0.98696 and 0.680699, respectively. The relative relation of λ_1 and λ_2 in the studied cases are summarized in Table 5.

5. Simulation with calibrated and adjusted sensitivity coefficients

With the values of the two calibrated sensitivity coefficients, and most importantly, their quantitative relationship calibrated from the field data, this section discusses the stability test against the FVD model as a representative symmetric car-

Table 3
Data screening criteria for car-following analysis of the ramp traffic.

Velocity	>=	5 ft/s
Spacing	<=	60 ft
Headway	<=	20 s
Velocity difference	>=	1 ft/s
Vehicle class		Auto

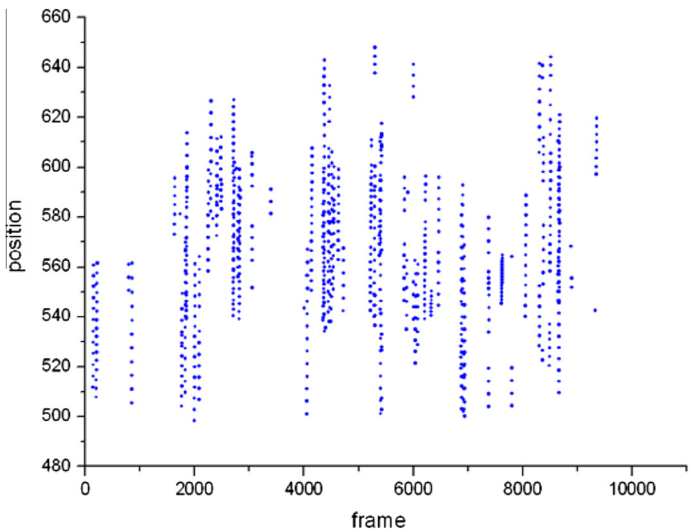

Fig. 4. The time space diagram of the on-ramp section.

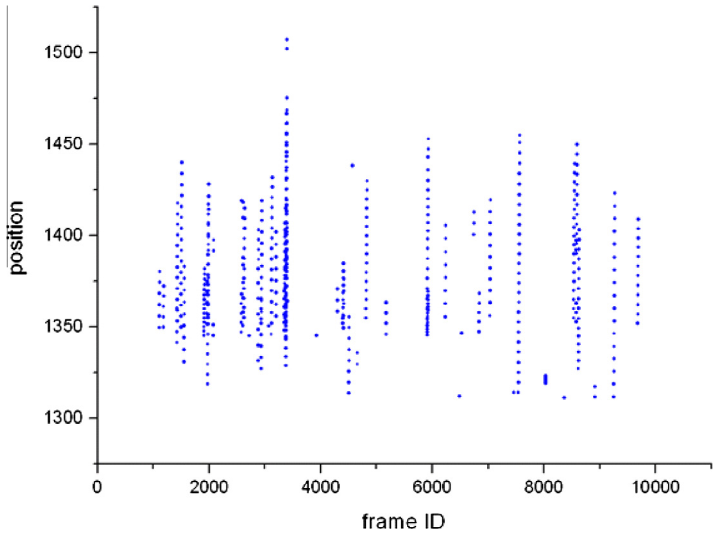

Fig. 5. The time space diagram of the off-ramp section.

Table 4
Calibration of the AFVD model from main lane and ramp data.

Lane 1	$\frac{dv_n(t)}{dt} = 0.415873[Tanh(1.80049\Delta x_n(t) - 10.1075) - v_n(t)] + 1.0824H(-\Delta v_n(t))\Delta v_n(t) + 0.69271H(\Delta v_n(t))\Delta v_n(t)$
Off-ramp	$\frac{dv_n(t)}{dt} = -1.26404v_n(t) + 0.997205H(-\Delta v_n(t))\Delta v_n(t) + 0.361254H(\Delta v_n(t))\Delta v_n(t)$
On-ramp	$\frac{dv_n(t)}{dt} = -0.881606(1 + v_n(t)) + 0.98696H(-\Delta v_n(t))\Delta v_n(t) + 0.680699H(\Delta v_n(t))\Delta v_n(t)$

Table 5
Relative relation between the two sensitivity coefficients in AFVD under dense and light traffic conditions.

Location	$\vert\lambda_1/\lambda_2\vert$
Main lane	1.56
Off-ramp	2.76
On-ramp	1.45

following approach, and the symmetric AFVD model. A simulation analysis was conducted, to which a set of sensitivity coefficients was applied for comparison. Simulation results in the form of stop-and-go charts were generated to demonstrate the differences between the models. Through the comparison, we can find a minor modification to existing car-following theories, as what the AFVD does, could lead to substantial change in model performance.

The mathematical representation of the simulation scheme could be expressed by:

$$\begin{cases} v_n(t+\Delta t) = v_n(t) + \Delta t \times \{\kappa[V(x_{n-1}(t) - x_n(t)) - v_n(t)] + \lambda_1[H(v_{n-1}(t) - v_n(t))][v_{n-1}(t) - v_n(t)] + \lambda_2[H(v_{n-1}(t) - v_n(t))][v_{n-1}(t) - v_n(t)]\} \\ x_n(t+\Delta t) = x_n(t) + \Delta t \times \frac{v_n(t)+v_n(t+\Delta t)}{2} \end{cases} \tag{23}$$

The initial position and velocity distribution are defined as the following, with $V(\Delta x) = V_1 + V_2 \tanh[C_1(\Delta x - l_c) - C_2]$, and L being the length of the circle in meters and N being the number of vehicles.

$$\begin{cases} \begin{cases} x_n(t=0) = 1 & if\ n = 1 \\ [x_n(t=0) = (n-1)L/N & if\ n > 1 \end{cases} \\ v_n(t=0) = V(L/N) \\ C_1 = 0.13, C_2 = 1.57, l_c = 5,\ N = 100,\ L = 1500 \end{cases} \tag{24}$$

The sensitivity coefficients calibrated from the NGSIM dataset in the foregoing section was first applied to the simulation. In the AFVD model, $\lambda_1 = 1.0824$, $\lambda_2 = 0.69271$ and $V_1 = 6.75$, $V_2 = 7.91$, $\kappa = 0.41$ are utilized, while in the FVD model in which only one sensitivity coefficient is applicable, an average λ, i.e., 0.87302 is used. Fig. 6 demonstrates the difference in the form of stop-and-go chart.

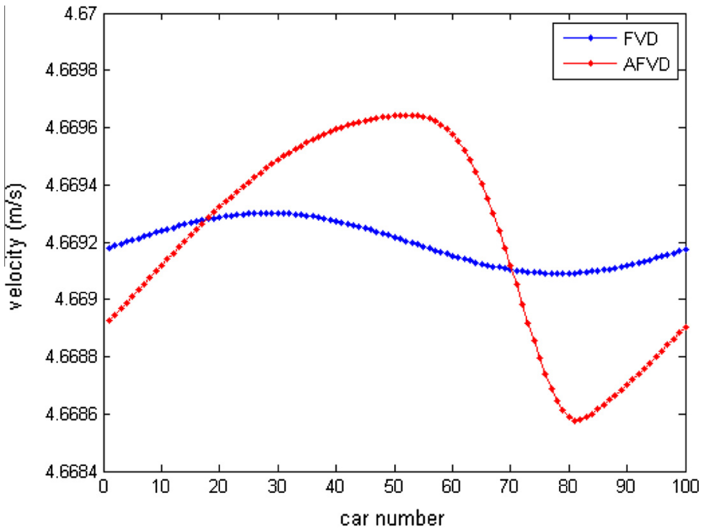

Fig. 6. Comparison of the stop-and-go charts of the FVD model and the AFVD model at 3000 s simulation time.

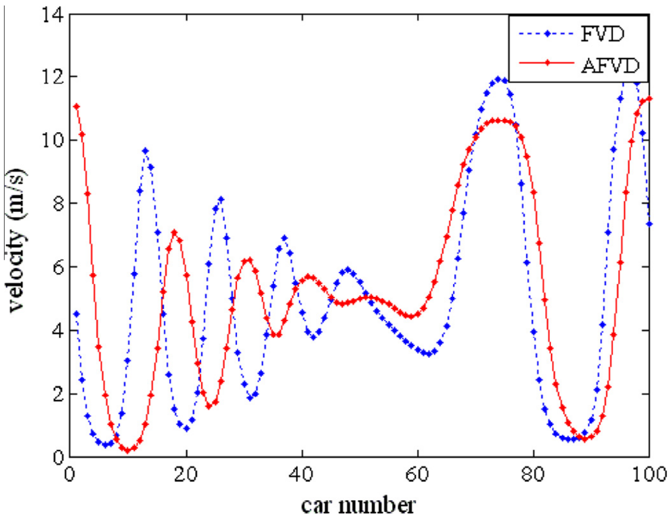

Fig. 7. Comparison of the stop-and-go charts of the FVD model and AFVD model at 300 simulation seconds.

The AFVD model's curve shows a shock wave frontier on the chart, while the FVD model does not show this phenomenon. While it is difficult to verify the phenomenon from the microscopic approach, if one extends the car-following approach to a continuum flow model, the shock waves could be better verified against field data. The necessity of precisely modeling the asymmetric characteristic at the microscopic level for explicitly explaining the formation and progression of shock waves has been discussed [1]. This result is a simple confirmation of that statement. Again, for a full scale evaluation, one can extend the AFVD car-following model to a macroscopic model. This way, the property of the AFVD based macroscopic flow model could be explicitly demonstrated through comparisons with classic continuum flow models and the filed data.

Hysteresis is often used to depict traffic conditions, as in [20,21]. In the second test, in order to show the differences in a better scale, hysteresis loops are developed with a new setting of $\lambda_1 = 0.6$, $\lambda_2 = 0.3$ in the AFVD model and $\lambda = 0.45$ in the FVD model. At different simulation times, i.e., 300 s and 2000 s, the stop-and-go chart and hysteresis loops are depicted in Figs. 7 and 8.

The FVD and AFVD models present different stability properties in Fig. 7 although the variance in velocity was found to be minimal. To get a better understanding, hysteresis loops were produced in Fig. 8. The hysteresis loops of the FVD model and AFVD model are similar in shape but slightly different in size and dimension. This implies the intensity difference in acceleration and deceleration may result in variance in the magnitude of hysteresis loops which, at macroscopic level, may lead to different patterns of congestion formation and propagation. This property has been further investigated by the authors in [1].

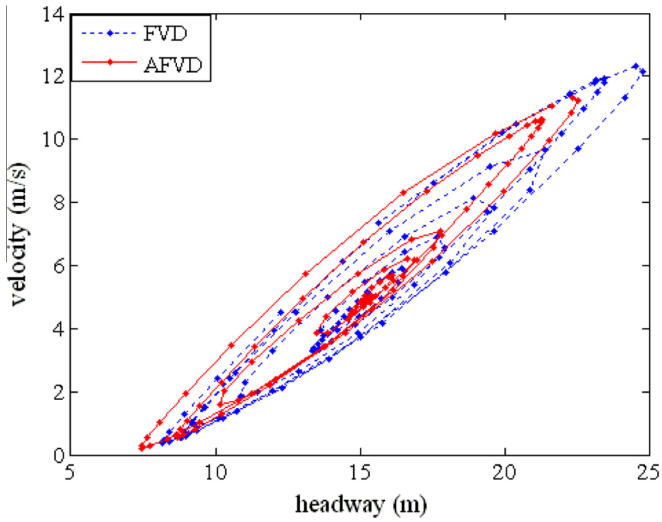

Fig. 8. Comparison of the hysteresis loops of the FVD model and AFVD model at 300 simulation seconds.

6. Conclusion

A microscopic car-following model was developed which considers the asymmetric acceleration and deceleration characteristic of vehicles. A higher order differential equation has been developed to take into account the impacts of acceleration and deceleration separately. A novel scheme was applied to solve the mathematical model and high resolution field data was used to calibrate the two sensitivity coefficients. The quantitative values of the two coefficients, and most significantly, the relative relationship between these two parameters have been extracted from collective traffic. It concludes that in the studied traffic flow, the relative intensity of deceleration and acceleration varies from 1.45 to 2.76 which fall into the range of $(1, 2.8)$. To further demonstrate the properties of the asymmetric model, the field calibrated parameters were then applied to the FVD and the AFVD model in a simulation environment to depict the impact of the asymmetric characteristic to traffic flow. Studies have been conducted to extend the AFVD approach into a continuum flow model from which the impacts of asymmetry to macroscopic traffic flow are revealed.

Reference

[1] H. Liu, H. Xu, H. Gong, Modeling the asymmetry in traffic flow (b): macroscopic approach, Appl. Math. Model. (2012). submitted for publication.
[2] D. Wei, H. Liu, Analysis of asymmetric driving behavior using a self-learning approach, Transp. Res. B Method. 46 (1) (2012) 1–14.
[3] H. Wang, K. Rudy, J. Li, D. Ni, Calculation of traffic flow breakdown probability to optimize link throughput, Appl. Math. Model. 34 (2010) 3376–3389.
[4] W. Gu, M. Cassidy, W. Li, On the capacity of highway checkpoints: models for unconventional configurations, Transp. Res. B Method. 46 (10) (2012) 1308–1321.
[5] R. Herman, E.W. Montroll, R.B. Potts, R.W. Rothery, Traffic dynamics: analysis of stability in car following, Oper. Res. 7 (1) (1959) 86–106.
[6] G.F. Newell, Nonlinear effects in the dynamics of car following, Oper. Res. 9 (2) (1961) 209–229.
[7] Z. Tian, M. Kyte, R. Troutbeck, W. Brilon, Implementing the maximum likelihood methodology to measure driver's critical gap, Transp. Res. Part A 33 (1999) 187–197.
[8] M. Bando, K. Hasebe, K. Nakanishi, A. Nakayama, Analysis of optimal velocity model with explicit delay, Phys. Rev. E 58 (5) (1998) 5429.
[9] D. Helbing, B. Tilch, Generalized force model of traffic dynamics, Phys. Rev. E 58 (1) (1998) 133.
[10] R. Jiang, Q. Wu, Z. Zhu, Full velocity difference model for a car-following theory, Phys. Rev. E 64 (1) (2001) 017101.
[11] H. Gong, H. Liu, B.H. Wang, An asymmetric full velocity difference car-following model, Phys. A Math. Theor. 387 (2007) 2595–2602.
[12] D. Vangi, A. Virga, Evaluation of emergency braking deceleration for accident reconstruction, Veh. Syst. Dyn. 45 (10) (2007) 895–910.
[13] H.M. Zhang, A mathematical theory of traffic hysteresis, Transp. Res. B Method. 33 (1) (1999) 1–23.
[14] T. Kim, H.M. Zhang, A stochastic wave propagation model, Transp. Res. B Method. 42 (7) (2008) 619–634.
[15] P. Ranjitkar, T. Nakatsuji, M. Asano, Performance evaluation of microscopic traffic flow models with test track data, Transp. Res. Rec. J. Transp. Res. Board 1876 (2004) 90–100.
[16] E. Brockfeld, R. Kühne, P. Wagner, Calibration and validation of microscopic traffic flow models, Transp. Res. Rec. J. Transp. Res. Board 1876 (2004) 62–70.
[17] V. Punzo, F. Simonelli, Analysis and comparison of microscopic traffic flow models with real traffic microscopic data, Transp. Res. Rec. J. Transp. Res. Board 1934 (2005) 53–63.
[18] S. Ossen, S. Hoogendoorn, Car-following behavior analysis from microscopic trajectory data, Transp. Res. Rec. J. Transp. Res. Board 1934 (2005) 13–21.
[19] M.E. Fouladvand, A.H. Darooneh, Statistical analysis of floating-car data: an empirical study, Eur. Phys. J. B 47 (2) (2005) 319–328.
[20] D.C. Gazis, Traffic Theory, Springer, 2002.
[21] S. Ahn, S. Vadlamani, J. Laval, A method to account for non-steady state conditions in measuring traffic hysteresis, Transp. Res. Part C (2011), http://dx.doi.org/10.1016/j.trc.2011.05.020.